RESEARCH ARTICLE

VOLCANICA

Biotite chemistry fingerprinting for Cenozoic ignimbrites and distal ash-fall correlation, southern Central Andean Volcanic Zone

Francisco Hevia-Cruz *[α,β,γ], José A. Naranjo[β], and Yuji Orihashi[δ]

[α] Departamento de Ciencias de la Tierra, Facultad de Ciencias Químicas, Universidad de Concepción, Concepción, Chile.
[β] Servicio Nacional de Geología y Minería (Sernageomin), Santiago, Chile.
[γ] Departamento de Geología, Facultad de Ciencias Físicas y Matemáticas, Universidad de Chile, Santiago, Chile.
[δ] Hirosaki University, 3 Bunkyo-cho, Hirosaki, Aomori, Japan.

Submitted: 2025-05-16 | Accepted: 2026-07-29 | Published: 2026-08-24

Editor: A. Jeffery | Production: A. Ryan

Abstract

Explosive eruptions can disperse ash over hundreds of kilometers, but correlating proximal ignimbrites with distal ash-fall deposits remains challenging when units have similar ages and field characteristics. We studied twelve ignimbrites in the southern Central Andean Volcanic Zone of northern Chile (25–27°S) using a combination of lithofacies observations, petrography, and mineral chemistry data. We evaluate biotite major-element chemistry as a fingerprinting tool for ignimbrite correlation and compare our results with published data from distal ash-fall deposits in the Coastal Cordillera (~350 km NW of potential sources). Biotite compositions define distinct fields for most units, distinguishing the Río Frío and Vega Helada ignimbrites despite similar lithofacies and ages. Pajonales and Juncalito ignimbrites show similar compositions, ages, and petrography, supporting a close correlation. One distal ash-fall deposit is correlated with the Laguna Verde Ignimbrite based on age and biotite chemistry, whereas another shows only tentative chemical affinity with the Wheelwright Ignimbrite.

Resumen

Las erupciones explosivas pueden dispersar ceniza a cientos de kilómetros, pero correlacionar ignimbritas proximales con depósitos distales es difícil cuando las unidades presentan edades y características similares. En la Zona Volcánica Central sur del norte de Chile (25–27°S), estudiamos las litofacies, petrografía y análisis de química mineral de doce ignimbritas. Evaluamos la química de elementos mayores de biotita para caracterizar ignimbritas y la comparamos con datos publicados de depósitos distales en la Cordillera de la Costa (~350 km al NW de sus fuentes potenciales). Las composiciones de biotita definen campos distintivos para la mayoría de las ignimbritas, diferenciando a Río Frío y Vega Helada pese a sus similitudes. Las ignimbritas Pajonales y Juncalito se correlacionan por composiciones, edades y petrografía similares. Un depósito distal se correlaciona con la ignimbrita Laguna Verde por su edad y química de biotitas, mientras otro muestra solo afinidad química con la ignimbrita Wheelwright.

Keywords: Ignimbrite fingerprinting; Biotite major-element chemistry; Lithofacies; Distal ash-fall correlation; Central Andean Volcanic Zone; Northern Chile.

1 Introduction

Explosive volcanic eruptions can disperse pyroclastic material over hundreds of kilometers, producing widespread proximal ignimbrites and distal ash-fall deposits. Establishing correlations between proximal and distal deposits is essential for reconstructing eruption magnitude, dispersal patterns, and assessing volcanic hazard, but it remains challenging when multiple units have similar field characteristics, overlapping age ranges, or incomplete exposure [e.g. Hildreth and Mahood 1985; Shane et al. 2003; Smith et al. 2011]. This is particularly relevant in the southern Central Andean Volcanic Zone (CVZ) of northern Chile, where numerous Cenozoic ignimbrites are exceptionally well preserved due to the extreme aridity of the Atacama region [e.g. Dunai et al. 2005].

The study area, located between ~25° and 27°S, contains a large assemblage of Neogene ignimbrites generated along the southern CVZ (Figure 1). Several of these deposits have been mapped and dated in previous regional studies, and their sources have been linked to large caldera systems in the high Andes [e.g. Clavero et al. 2012; Naranjo et al. 2013a; b; 2016; Naranjo et al. 2018; Naranjo et al. 2019]. However, correlation among these units remains difficult in some cases because several ignimbrites share similar field and lithofacies characteristics, including color, petrographic assemblages, welding grade, pumice abundance and textures, and overlapping published age ranges. These similarities are particularly problematic where lateral continuity is poor, outcrops are isolated, or radiometric ages alone do not provide enough resolution. Such ambiguities highlight the need for correlation tools that complement field relationships, lithofacies observations, petrography, and geochronology.

In this context, mineral chemistry provides an effective approach for fingerprinting pyroclastic deposits, especially when glass is altered, absent, or difficult to compare among proximal and distal deposits. Biotite has been widely used for ignimbrite and tephra correlation because it commonly survives transport and alteration, can be analyzed in both proximal and distal deposits, and may retain compositional differences among eruptive units [e.g. Hildreth and Mahood 1985; de Silva and Francis 1989; Lindsay et al. 2001; Shane et al. 2003; Folkes et al. 2011; Smith et al. 2011; Breitkreuz et al. 2014; Sliwinski et al. 2017]. In the Central Andes, biotite chemistry has been

* franciscohevia@udec.cl

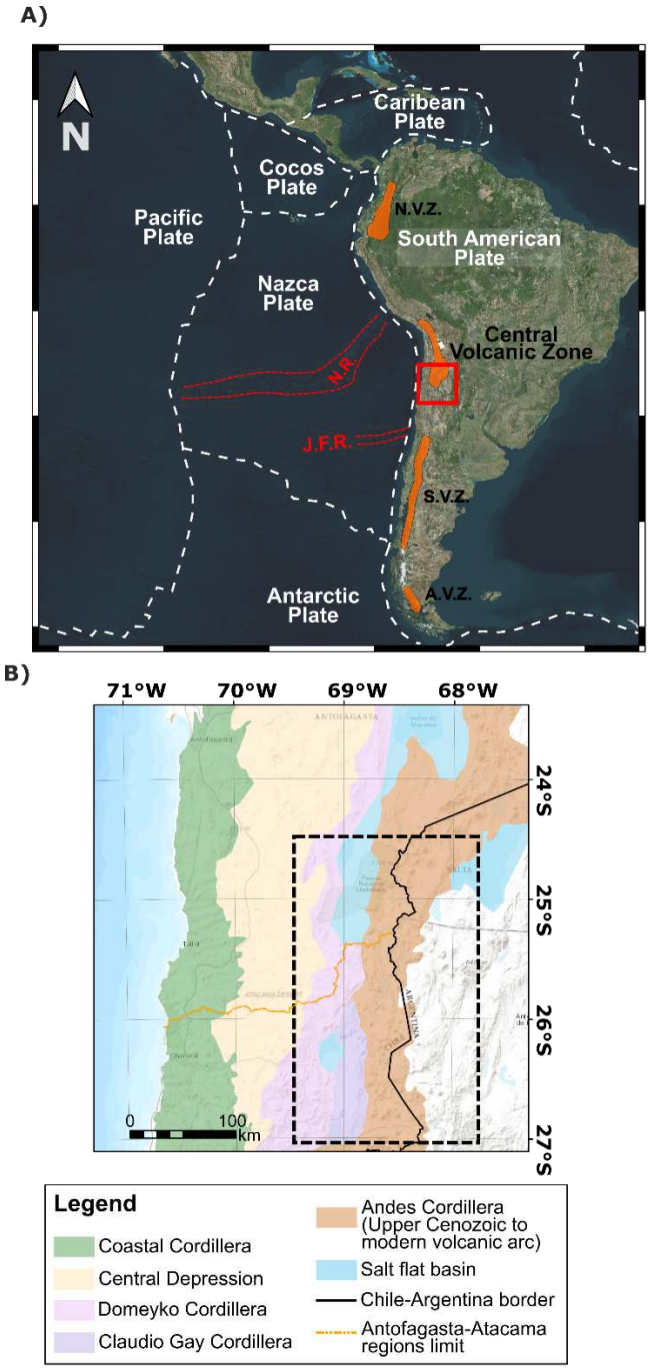


Figure 1: Location and geological context of the study area. [A] Tectonic setting of South America and Andean Volcanic Zones distribution. N.R.: Nazca Ridge; J.F.R.: Juan Fernández Ridge; N.V.Z., S.V.Z. and A.V.Z.: Northern, Southern and Austral Volcanic Zones, respectively. Modified after Stern [2004]. The red square corresponds to the inset presented in [B], which shows the main geographic features of northern Chile (and northwestern Argentina). The dashed rectangle corresponds to the approximate study area. The different "Cordilleras" correspond to chains of the Andes range with distinct age ranges and associated to different fault systems [e.g. Naranjo et al. 2018, and references therein], with the "Andes Cordillera" the modern volcanic arc. The back-arc (northern Pampean Ranges) is uncolored (white and pale greys).

particularly useful for correlating large ignimbrites and distal ash deposits where field continuity is lacking [e.g. de Silva and Francis 1989; Lindsay et al. 2001; Breitkreuz et al. 2014].

Here, we evaluate major-element biotite chemistry as a fingerprinting tool for twelve Neogene ignimbrites from the southern CVZ of northern Chile. We combine Electron Probe Microanalysis (EPMA) of biotite crystals with selected lithofacies and petrographic observations to test correlations among proximal ignimbrite units and to compare our dataset with published biotite data from distal ash-fall deposits in the Coastal Cordillera near Antofagasta, ~350 km northwest of potential sources [Breitkreuz et al. 2014]. Our main goals are to: (1) assess whether biotite chemistry can distinguish ignimbrites with similar field characteristics and ages; (2) evaluate the previously proposed correlation between the Pajonales and Juncalito ignimbrites; and (3) test possible correlations between southern CVZ ignimbrites and distal ash-fall deposits along the northern Chilean coast.

1.1 Geological Context

The study area is located in the southern CVZ of northern Chile, between ~25° and 27°S. This segment of the Andean volcanic arc is related to the subduction of the Nazca Plate beneath the South American Plate (Figure 1A; Stern 2004) and hosts numerous Neogene volcanic centers, calderas, and large-volume ignimbrite deposits. The studied ignimbrites are mostly exposed immediately west of the modern volcanic arc, although some deposits extend several tens to hundreds of kilometers westward through valleys and intermontane basins [Naranjo et al. 2018, and references therein].

From west to east, the main morphostructural domains crossed by these deposits are the Coastal Cordillera, Central Depression, Domeyko Cordillera, Claudio Gay Cordillera, and the high Andes volcanic arc (Figure 1B). The Coastal Cordillera, where distal ash-fall deposits have been described near Antofagasta [Breitkreuz et al. 2014], lies along the Pacific margin. Farther east, the Domeyko and Claudio Gay cordilleras form intermediate topographic barriers between the Central Depression and the volcanic arc. The high Andes host the calderas and volcanic centers that generated the ignimbrites studied here.

The region contains a well-preserved Neogene ignimbrite record, favored by the extreme aridity of the Atacama Desert [e.g. Dunai et al. 2005]. These deposits were mapped and described in previous geological studies, which identified their approximate distribution, stratigraphic relationships, age ranges, and probable source calderas [e.g. Seggiaro et al. 2006; Seggiaro et al. 2007; Clavero et al. 2012; Naranjo et al. 2013a; b; 2016; Naranjo et al. 2018; Naranjo et al. 2019]. The main units considered in this study include, from older to younger, the Antiguas, Río Frío, Vega Helada, Pajonales, Juncalito, Salar Grande, Barrancas Blancas, San Andrés, Los Colorados, Wheelwright, Parinas, and Laguna Verde ignimbrites. Their known distribution is summarized in Figure 2, and their published age ranges, source assignments, and main correlation

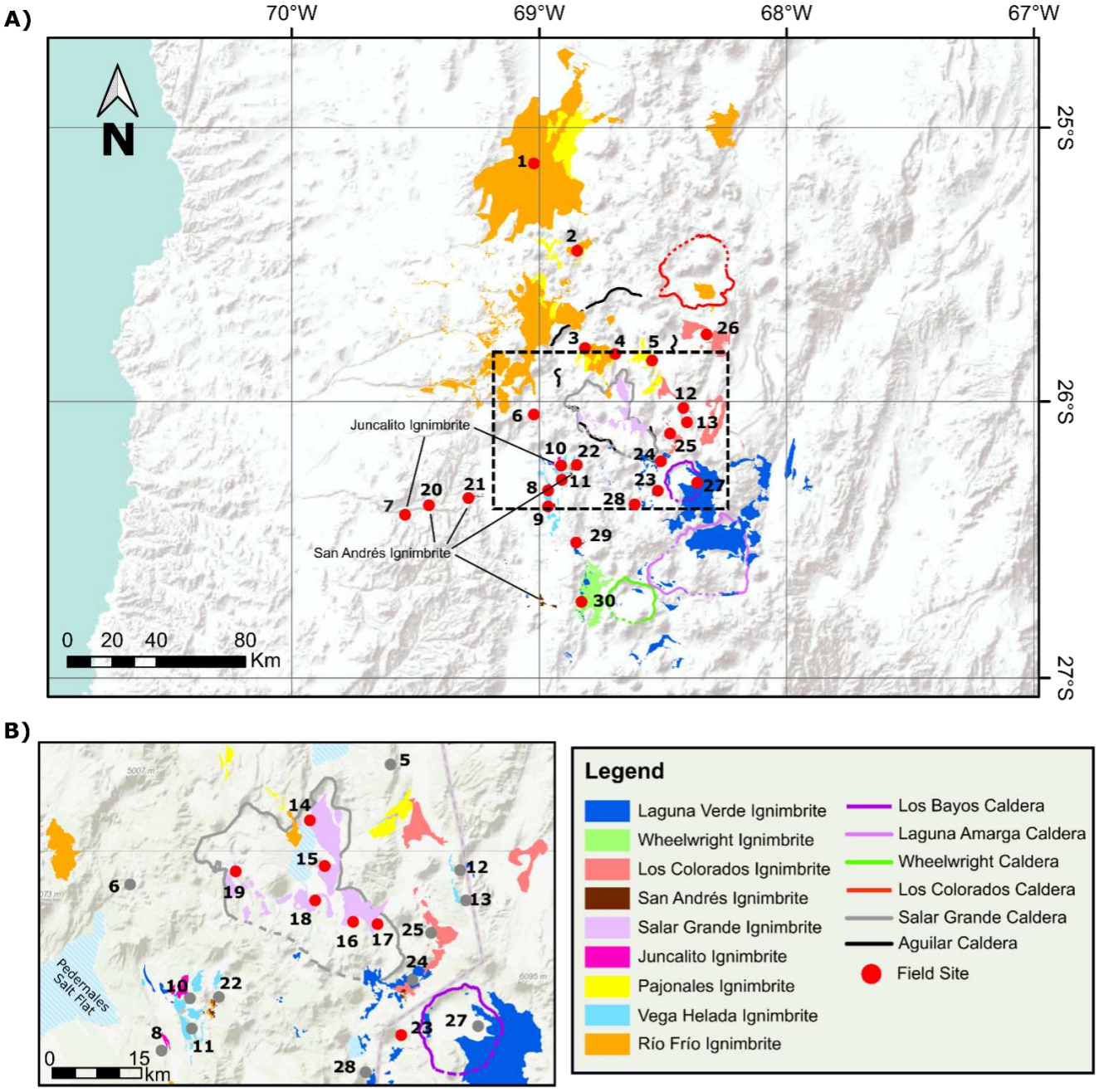


Figure 2: [A] Distribution of the studied ignimbrites, indicated with different colors, San Andrés and Juncalito are indicated directly in the figure due to their limited outcrop distribution. [B] corresponds to the inset of the dashed rectangle in [A]. The gray circles in [B] indicate the sites already shown in [A]. The Barrancas Blancas ignimbrite crops out at the base of site 24 and the Parinas ignimbrite occurs near field site 12. The Antiguas ignimbrites are not represented because they do not correspond to a single mapped ignimbrite unit, but rather to a group of older, undifferentiated ignimbrites used here as a geochemical baseline. Modified after Seggiaro et al. [2006], Seggiaro et al. [2007], Clavero et al. [2012], Naranjo et al. [2013a,b, 2016], Naranjo et al. [2018], and Naranjo et al. [2019].

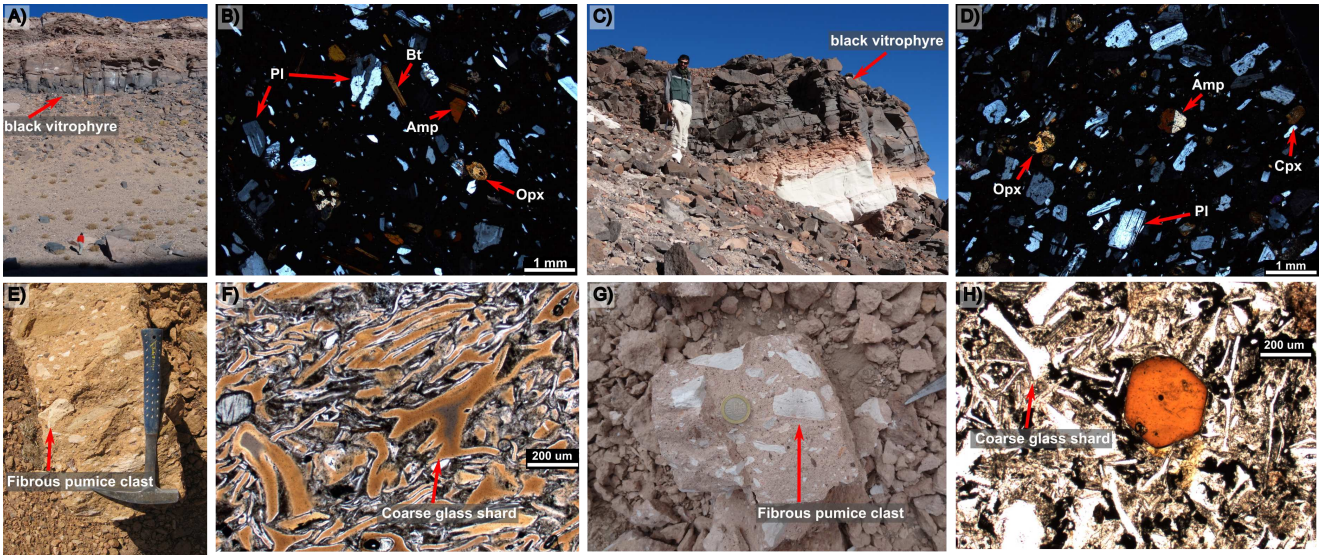


Figure 3: Characteristic macro- and microscopic features of the Río Frío (RF-2), Vega Helada (VH-2), Pajonales (PAJ-3), and Juncalito (Junc-2) ignimbrites. [A] Field photograph of the Río Frío ignimbrite (RF-2), showing welded crystal lapilli-tuff layers, including a black vitrophyre. [B] Thin section of RF-2 with plagioclase, orthopyroxene, amphibole, and scarce biotite in a glassy matrix. [C] Field photograph of the Vega Helada ignimbrite (VH-2), likewise displaying variations in welding grade, including in a vitrophyre. [D] Thin section of VH-2 with plagioclase, clinopyroxene, orthopyroxene, and scarce amphibole in a glassy matrix. [E] Hand specimen of the Pajonales ignimbrite (PAJ-3) with characteristically abundant fibrous pumice fragments. [F] Thin section of PAJ-3 showing scarce phenocrysts in a coarse, glass shard-rich matrix. [G] Hand specimen of the Juncalito ignimbrite (Junc-2) with abundant fibrous pumice fragments. [H] Thin section of Junc-2 with sparse phenocrysts in a coarse, glass shard-rich matrix. Mineral abbreviations follow Whitney and Evans [2010]: Pl = plagioclase, Amp = amphibole, Bt = biotite, Opx = orthopyroxene, Cpx = clinopyroxene.

issues are compiled in Table 1. The Antiguas, Barrancas Blancas, and Parinas ignimbrites are not shown in Figure 2 because of their limited outcrop extent at the map scale, but their occurrence in the studied sections is documented in the stratigraphic columns of Supplementary Material Appendix A1. Available regional whole-rock data indicate that these ignimbrites are predominantly silicic, ranging mostly from dacitic/rhyodacitic to rhyolitic compositions, although comparable whole-rock analyses are not available for all units and bulk ignimbrite samples may include variable proportions of juvenile material, crystals, matrix, and lithic fragments [Siebel et al. 2001; Schnurr et al. 2007].

The oldest units considered here are grouped as the Antiguas Ignimbrites, with reported ages between ~25 and 22 Ma and poorly constrained sources. They are followed by the lower Miocene Río Frío and Vega Helada ignimbrites (~19–17 Ma and ~19 Ma, respectively), which show similar field and petrographic characteristics in some localities but might have different source interpretations. The Pajonales and Juncalito ignimbrites are both ~16 Ma units with comparable pumice-rich facies and overlapping published age ranges. Middle to upper Miocene units include the Salar Grande, Barrancas Blancas, San Andrés, and Los Colorados ignimbrites, whereas the youngest studied units are the Wheelwright, Parinas, and Laguna Verde ignimbrites, with published ages between ~5 and 3 Ma (Table 1).

Despite previous mapping and geochronological work [e.g. Clavero et al. 2012; Naranjo et al. 2013a; b; 2016], several units remain difficult to correlate because of similar lithofacies, discontinuous exposure, overlapping radiometric ages, or uncertain source areas. These difficulties are especially relevant for distinguishing physically similar ignimbrites in proximal and medial areas, and for testing possible links between Andean ignimbrites and distal ash-fall deposits preserved in the Coastal Cordillera. Therefore, in this study, published stratigraphic and geochronological constraints are used as an independent framework to evaluate the usefulness of biotite chemistry for ignimbrite fingerprinting and distal ash correlation.

2 Methods and Materials

This study combines field, petrographic, geochronological, and mineral chemistry data to evaluate biotite chemistry as a fingerprinting tool for ignimbrite correlation. Field and petrographic observations were used to verify unit assignments, document diagnostic features, and identify cases where lithofacies similarities preclude correlation. Biotite major-element chemistry was then used to test correlations among proximal ignimbrites and with published data from distal ash-fall deposits.

2.1 Field, Petrographic, and Stratigraphic Constraints

This study systematizes field information collected over several years during regional geological mapping campaigns, including two field campaigns conducted in 2014 and 2015 and previous mapping work in the Salar de Pajonales–Cerro Moño, Salar de Aguilar–Portezuelo del León Muerto, and

Table 1: Summary of the studied ignimbrites, including published age ranges, main correlation issues, probable source calderas, and key references.

Epoch	Ignimbrite	Published age range (Ma)	Main correlation issue	Probable source (caldera)	Key references
Pliocene	Laguna Verde	~5–3	Well-exposed and widely distributed ignimbrite, locally close to the Los Colorados and San Andrés ignimbrites, with which it shares some field characteristics, including pale pink colors and millimeter-scale glass shards.	Laguna Escondida, Laguna Amarga, Peinado	Clavero et al. [1997] and Naranjo et al. [2018]
	Parinas	~5	Similar age range to Wheelwright and Laguna Verde, with facies locally resembling some Wheelwright deposits, including brownish tones and abundant vitreous pumice; it is commonly poorly preserved due to low welding grade.	Alto Parinas	Naranjo and Cornejo [1992]
	Wheelwright	~5–4	Similar age range to Laguna Verde and Parinas, and locally similar facies to Parinas.	Wheelwright	Clavero et al. [2012]
Upper Miocene	Los Colorados	~10–8	Welded ignimbrite with abrupt changes in welding grade over short distances, complicating field identification. Its outcrops are also located near the Chile–Argentina border, limiting direct lateral tracing. Its age range partly overlaps those of Barrancas Blancas and San Andrés.	Los Colorados	Seggiaro et al. [2006] and Naranjo et al. [2019]
	San Andrés	~10–9	Locally occurs near Barrancas Blancas and Laguna Verde and can show similar pale pink colors and macroscopic features. Its age range is also close to those of Los Colorados and Barrancas Blancas.	Pampa de los Bayos	Clark et al. [1967], Naranjo et al. [2016], and Naranjo et al. [2018]
	Barrancas Blancas	~9.3	Very similar to San Andrés in macro- and microscopic petrographic features, with a comparable age. It is exposed at a single locality, where it is clearly eroded and overlain by San Andrés.	Barrancas Blancas	Clavero et al. [1997], Naranjo et al. [2016], and Naranjo et al. [2018]
Middle Miocene	Salar Grande	12–11	Mostly preserved as intracaldera deposits and with ages not closely overlapping other units, so it presents no major regional correlation problems. Locally, however, some poorly welded, pumice- and lithic-rich facies may resemble Juncalito.	Salar Grande	Naranjo and Cornejo [1992] and Naranjo et al. [2013a]
Lower Miocene	Juncalito	~16	Strong lithofacies, petrographic, distribution, and age similarity with Pajonales.	Unknown	Clavero et al. [1997]
	Pajonales	~16	Strong lithofacies, petrographic, distribution, and age similarity with Juncalito.	Aguilar	Naranjo and Cornejo [1992], Naranjo et al. [2013b], and Naranjo et al. [2018]
	Vega Helada	~19	Similar lithofacies and age range to Río Frío.	Unknown	Clavero et al. [1997]
	Río Frío	19–17	Widely distributed ignimbrite with highly welded facies similar to those of several other units, such as Los Colorados. It is especially similar to Vega Helada in terms of facies, macro- and microscopic petrography, distribution, and published age range.	Aguilar	Naranjo and Puig [1984], Siebel et al. [2001], and Naranjo et al. [2018]
	Antiguas	25–22	Older isolated units; used as a geochemical baseline, no source identified.	Unknown	Naranjo et al. [2013a,b, 2016]

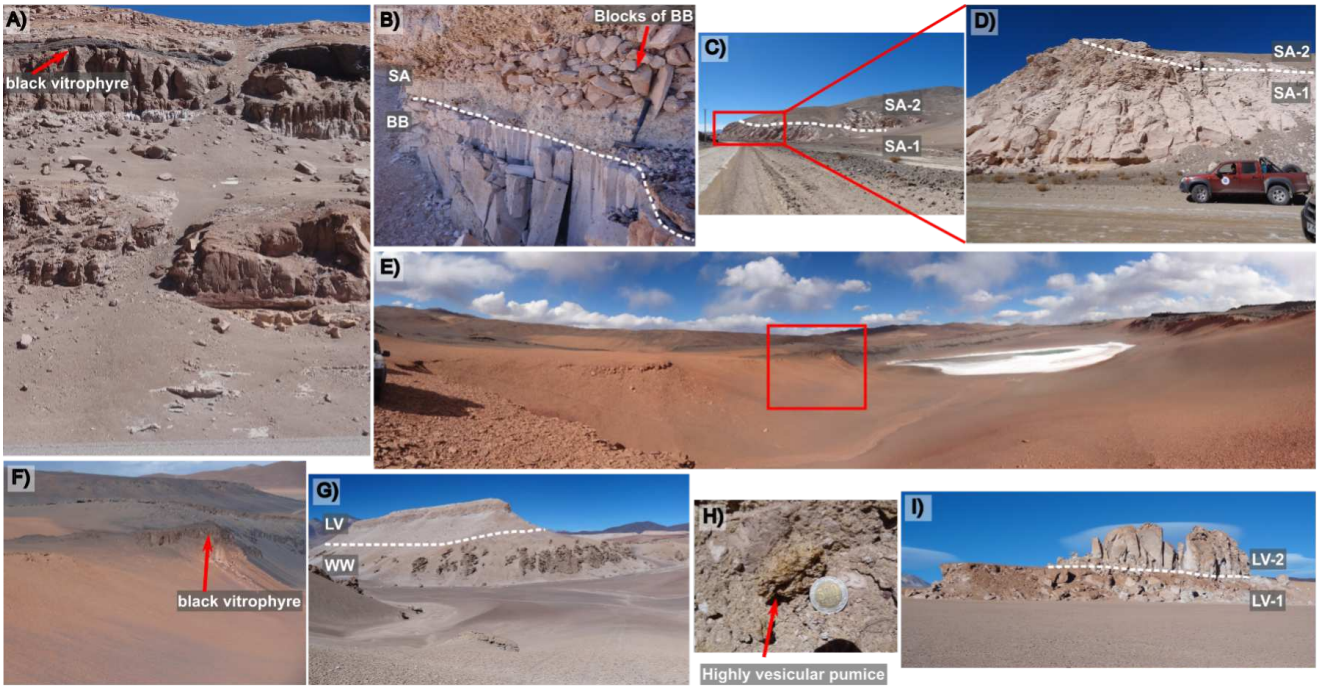


Figure 4: Field photographs of the Salar Grande (SG), Barrancas Blancas (BB), San Andrés (SA), Los Colorados (COL), Wheelwright (WW), and Laguna Verde (LV) ignimbrites. [A] SG showing marked variation in welding grade, including a black vitrophyre. [B] Erosive contact between BB and SA; BB displays columnar jointing and the basal part of SA incorporates fragments derived from BB columnar-jointed blocks. [C]–[D] SA with two flow units (SA-1 and SA-2). [E]–[F] COL illustrating the transition from its characteristic red, weakly to moderately welded facies to a black vitrophyre. The red rectangle in E corresponds to an inset of F. [G] Contact between WW and LV. [H] WW hand specimen with characteristic pumice clasts showing large vesicles. [I] LV showing two flow units (LV-1 and LV-2).

Cerro Panteón de Aliste–Cerro Colorado areas [Naranjo et al. 2013a; b; 2016]. The compiled dataset includes observations from more than 400 localities, field photographs, macroscopic descriptions from field notebooks, and stratigraphic relationships. We complemented this information with new detailed petrographic descriptions of more than 200 thin sections and a similar number of hand specimens, together with an exhaustive compilation of published radiometric ages for the studied units.

Hand specimens and thin sections were examined using a hand lens, binocular microscope, and optical microscope at SERNAGEOMIN laboratories, Chile. Petrographic observations focused on features useful for correlation, including pumice type, welding grade, crystal assemblage, shard size and morphology, lithic abundance, and glomeroporphyritic textures. Lithofacies terminology follows Branney and Kokelaar [2002]. Stratigraphic columns and field relationships were reconstructed using a combination of field observations, Google Earth Pro imagery, ArcGIS Desktop 10.5.1, SedLog, Adobe Illustrator, and Inkscape. Detailed stratigraphic columns, field photographs, and petrographic descriptions are provided in Supplementary Material Appendix A1, whereas only the features directly relevant to the correlations are summarized in the main text. These datasets were used to evaluate lithofacies, stratigraphic relationships, lateral continuity, and outcrop distribution.

2.2 Biotite Sample Selection and Preparation

Biotite was selected because it is present in all the studied ignimbrites and has been widely used for correlation of ignimbrites and tephra deposits [e.g. de Silva and Francis 1989; Lindsay et al. 2001; Shane et al. 2003; Folkes et al. 2011; Smith et al. 2011; Breitkreuz et al. 2014]. Indeed, petrographic observations indicate that biotite is present in all the studied ignimbrites, although it is generally a minor to accessory phase within crystal assemblages dominated by plagioclase and, depending on the unit, amphibole, pyroxene, and/or quartz. Systematic modal point-counting was not performed for all samples; therefore, we report mineral abundances qualitatively rather than as directly comparable modal percentages. Available semi-quantitative estimates indicate variable total crystal contents, from crystal-poor pumice- and shard-rich facies in units such as Pajonales and Juncalito to crystal-rich facies in Río Frío, locally reaching ~40 % crystals or more, mostly plagioclase and pyroxenes. Samples were selected from localities where unit assignment was well constrained by field relationships, petrography, and published stratigraphy. Additional samples from ambiguous localities were included to test whether biotite chemistry could help resolve uncertain correlations.

Sample preparation was conducted at SERNAGEOMIN laboratories. Selected samples were crushed and sieved to obtain fractions enriched in biotite crystals, mainly between 0.125 and 2 mm, based on previous petrographic observations.

Biotite crystals were first concentrated using magnetic separation and then further enriched by repeated manual passes of the sieved fraction over paper, to which biotite flakes preferentially adhered. No hand-picking of individual crystals was performed. The resulting biotite concentrates were mounted in epoxy resin briquettes. The mounts were cut and polished to expose the crystals. The samples were further polished with diamond paste and carbon-coated to improve conductivity at the Earthquake Research Institute of the University of Tokyo, Japan.

2.3 EPMA Biotite Chemistry and Data Treatment

Major- and minor-element compositions of biotite were obtained by EPMA at the Earthquake Research Institute of the University of Tokyo, Japan, using a JEOL JXA-8800R equipped with five wavelength-dispersive spectrometers. The analyzed elements were Si, Ti, Al, Fe, Mn, Mg, Ca, Na, K, F, and Cl, and results are reported as weight percent oxides.

Analyses were performed with an accelerating voltage of 15 kV, a beam current of 12 nA, and a beam diameter of 5 µm. Instrument calibration and analytical performance were checked before each analytical session using the laboratory reference standard set routinely employed for silicate mineral analysis at the Earthquake Research Institute, University of Tokyo. A total of 35 biotite separates were analyzed, with an average of ~15 crystals per sample and commonly 2–3 spot analyses per crystal, exceptionally up to 10 spots in larger crystals. Because most crystals were small relative to the beam size, core–rim traverses were not performed systematically. Instead, spot analyses targeted well-exposed, inclusion-free and fracture-free crystal domains. In total, more than 1,200 spot analyses were obtained. Crystal-mean values were used for fingerprinting, and analyses with internal variability greater than 5 % within a single crystal were excluded from the fingerprinting dataset.

Structural formulas were calculated on the basis of 22 oxygen atoms following mica nomenclature conventions [Speer 1984; Deer et al. 1992; Rieder et al. 1998], and Fe^{3+} was estimated following Droop [1987].

3 Results

3.1 Field and Petrographic Constraints for Unit Correlation

Field and petrographic observations were used primarily to support unit assignment and to identify cases where physical similarities, such as lithofacies, color, distribution and/or petrography, complicate correlation. Detailed lithofacies descriptions, stratigraphic column correlations, field photographs, and thin-section images are provided in Supplementary Material Appendix A1. Here, we summarize only the field and petrographic features directly relevant to the correlation issues addressed in this study.

The Río Frío and Vega Helada ignimbrites are among the most difficult units to distinguish in the field. Both include pale grey to white lapilli-tuff facies that pass upward into dark, strongly welded to vitrophyric levels (Figure 3A,C). They also share broadly similar petrographic assemblages, including plagioclase, biotite, amphibole, and pyroxene in a glassy matrix with variable glass-shard contents (Figure 3B,D). Their age ranges partly overlap, further complicating correlation based only on field criteria and geochronology (Table 1).

The Pajonales and Juncalito ignimbrites also share several diagnostic field and petrographic features. Both are characterized by abundant fibrous pumice, low crystal contents dominated by plagioclase and biotite, and coarse glass-shard-rich matrices (Figure 3E–H). Their ages overlap around ~16 Ma (Table 1), and both units include pumice-rich, weakly to moderately welded facies. These similarities make their distinction uncertain in some localities and provide a key test case for biotite-chemistry fingerprinting.

The remaining studied ignimbrites were characterized to ensure reliable sample assignment before geochemical comparison. Their diagnostic features are summarized in Table 1 and documented in Supplementary Material Appendix A1. Among these units, Salar Grande, Barrancas Blancas, San Andrés, and Los Colorados (Figure 4A–F) provide additional regional reference fields for evaluating the discriminatory power of biotite chemistry. The Pliocene Wheelwright, Parinas, and Laguna Verde ignimbrites (Figure 4G–I) are particularly relevant for comparison with published distal ash-fall deposits from the Coastal Cordillera, because their age ranges overlap those of some distal deposits reported by Breitkreuz et al. [2014].

3.2 Biotite Major-Element Chemistry

The major-element chemistry of biotite crystals, expressed as weight percent oxides, is presented in Supplementary Material Table ST2. No consistent intra-crystal compositional trends were observed within analytical uncertainty. These data were used to evaluate whether each ignimbrite defines a distinctive compositional field. For unit fingerprinting, oxide concentrations in weight percent are plotted against SiO_2 to facilitate comparison among the studied units and with published datasets. Structural-formula parameters, including atoms per formula unit (a.p.f.u.), are used only where required for mineral classification or comparison with published data.

Na_2O and CaO are not shown in the main diagrams because their contents in biotite are generally low and highly scattered. Overall, most ignimbrites are compositionally homogeneous within each unit, although the degree of dispersion varies among units (Figure 5, Figure 6, Figure 7). Vega Helada and Los Colorados show the greatest within-unit compositional variability, whereas several other units, including Salar Grande, Barrancas Blancas, San Andrés, Wheelwright, Parinas, and Laguna Verde, form more restricted fields. The compositional ranges summarized in Table 2 correspond to the main clusters of analyses for each unit, excluding isolated outliers.

The lower Miocene ignimbrites show contrasting compositional patterns (Figure 5). Río Frío forms a relatively constrained compositional field for most oxides, whereas Vega Helada is more dispersed and is characterized by higher FeO and MnO and lower SiO_2 contents. Pajonales and Juncalito show broadly overlapping biotite compositions, particularly in FeO, MgO, TiO_2, Al_2O_3, and K_2O.

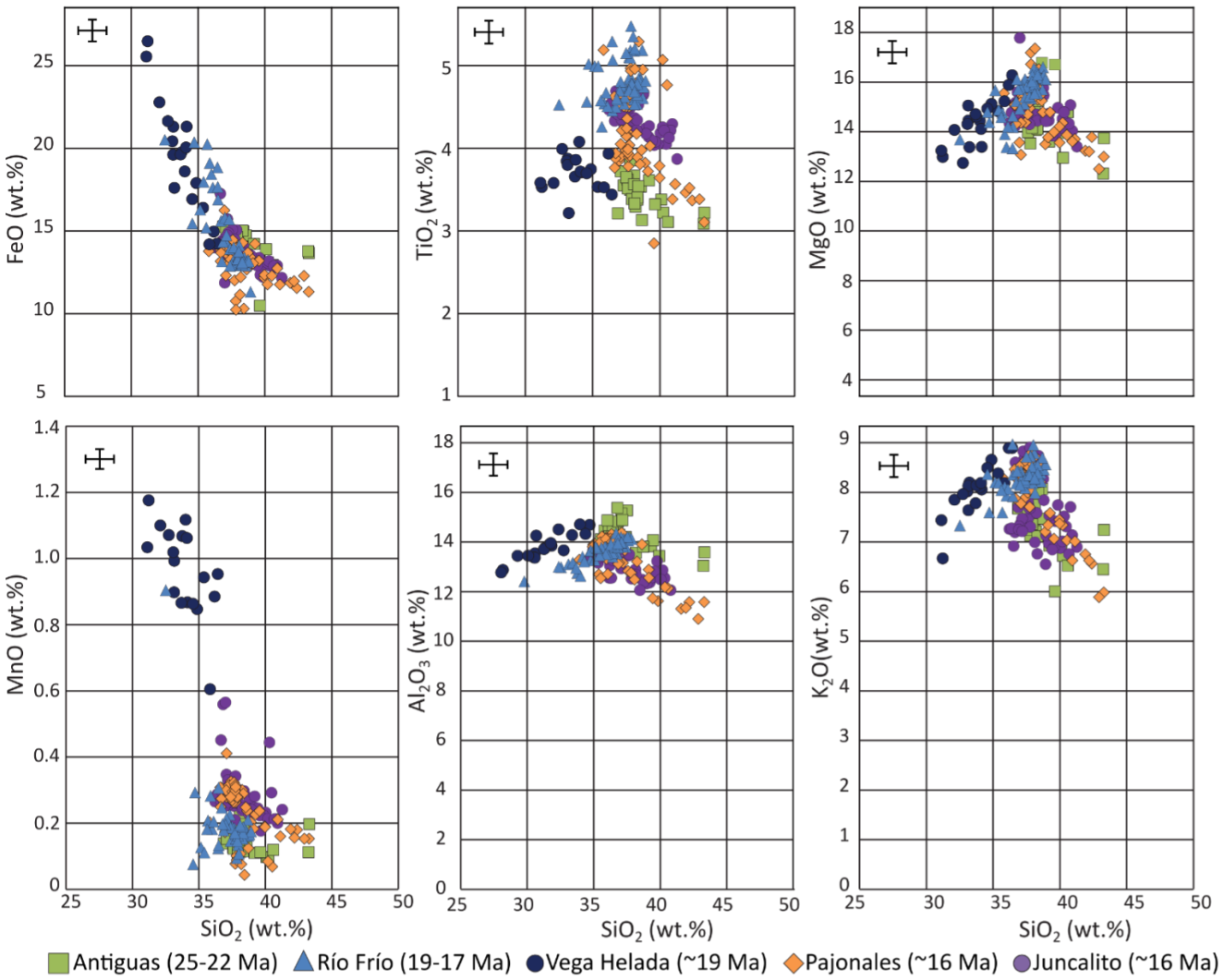


Figure 5: Distribution of different major elements as a function of silica content, expressed as weight percentage of oxides (wt.%), for biotite analyses from the Antiguas, Río Frío, Vega Helada, Pajonales, and Juncalito ignimbrites. Bars in the upper-left corner of each graph represent maximum estimated uncertainties.

Table 2: Compositional ranges of biotite geochemistry from the studied ignimbrites (in decreasing age), expressed as analyzed weight percentage of oxides. The ranges do not cover the entire spectrum of obtained values but are limited to the clusters that include most analyses for each unit.

Ignimbrite	SiO_2	FeO	TiO_2	MgO	MnO	Al_2O_3	K_2O
Antiguas	36.8–39.6	14.5–15.2	3.1–3.8	12.9–15.2	0.08–0.23	13.3–15.1	6.5–8.5
Río Frío	36.7–38.9	12.9–14.1	4.53–4.85	15.2–16.6	0.1–0.3	12.5–14.2	8.2–9.0
Vega Helada	32.7–35.4	17.0–21.3	3.4–4.0	13.2–15.2	0.84–1.18	12.8–14.7	7.6–8.9
Pajonales	36.7–38.2	13.0–14.3	3.9–4.7	14.9–15.9	0.26–0.32	13.2–14.3	8–8.7
Juncalito	36.2–39.2	12.9–15.0	4.0–4.7	14.0–16.0	0.20–0.34	12.3–14.1	6.8–8.8
Salar Grande	36.3–39.3	12.7–15.5	3.8–4.8	14.5–16.3	0.2–0.4	13.2–14.8	6.5–9.0
Barrancas Blancas	36.25–37.0	16.2–17.0	3.9–4.8	13.4–14.0	0.34–0.41	14.3–15.2	8.35–9.17
San Andrés	36.0–37.5	16.7–17.8	3.6–4.1	12.0–13.2	0.62–0.73	14.6–16.2	8.65–9.10
Los Colorados	35.0–39.0*	13.5–22.0*	3.3–4.5*	11.7–14.1*	0.3–0.8*	12.7–15.3*	6.1–9.0*
Wheelwright	36.8–37.9	16.5–17.5	4.1–4.6	13.5–14.3	0.31–0.36	13.4–14.4	8.6–9.0
Parinas	36.8–37.8	15.2–16.3	3.25–3.54	13.5–14.3	0.25–0.32	14.3–15.2	8.2–8.5
Laguna Verde	36.2–37.9	14.4–16.3	3.9–4.4	13.5–15.2	0.25–0.3; 0.5–0.54	13.1–14.6	8.0–8.9

*The Los Colorados Ignimbrite exhibits very high variability and does not have a representative composition range.

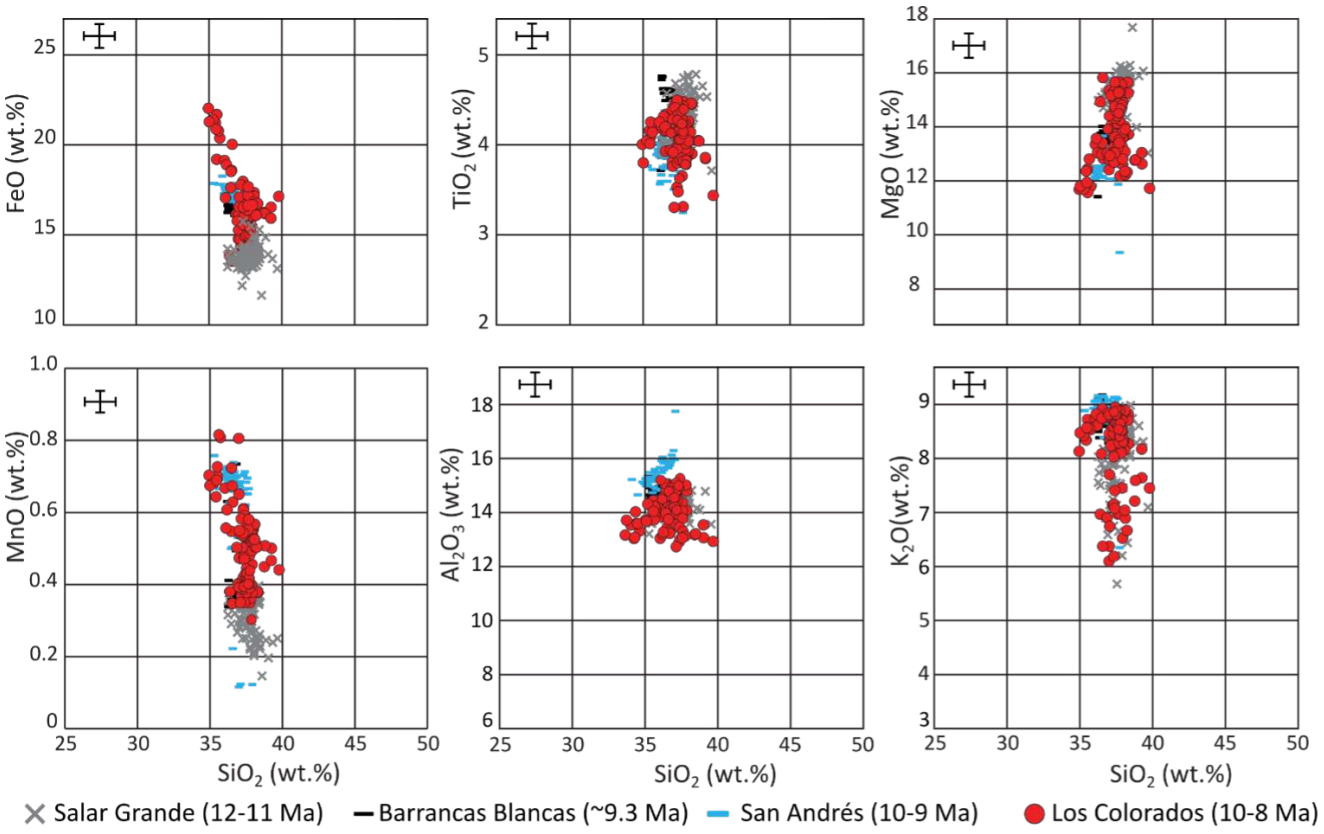


Figure 6: Distribution of different major elements as a function of silica content, expressed as weight percentage of oxides (wt.%), for biotite analyses from the Salar Grande, Barrancas Blancas, San Andrés, and Los Colorados ignimbrites. Bars in the upper-left corner of each graph represent maximum estimated uncertainties.

The middle to upper Miocene ignimbrites generally define more restricted fields, except for Los Colorados, which shows the highest internal variability and therefore lacks a single representative compositional range (Figure 6, Table 2). Salar Grande, Barrancas Blancas, and San Andrés define comparatively distinct compositional fields, although some overlap occurs in individual oxide plots.

The Pliocene ignimbrites Wheelwright, Parinas, and Laguna Verde also show relatively well-constrained biotite compositions (Figure 7). Laguna Verde defines a coherent field, although a secondary low-K_2O group is present. Wheelwright and Parinas have partly similar age ranges and some comparable field characteristics, but their biotite compositions differ in several major-element plots.

4 Discussion

4.1 Biotite Chemistry as a Fingerprinting Tool

The results presented above allow us to evaluate whether biotite major-element chemistry can be used as a fingerprinting tool to distinguish and correlate ignimbrites in the southern CVZ. In this study, no single oxide or diagram was used as a standalone criterion for correlation. Instead, geochemical matches are considered robust only when biotite compositions overlap consistently across multiple major-element diagrams and are supported by independent constraints such as published age ranges, field relationships, petrographic features, and geographic or stratigraphic position. Conversely, geochemical similarity in only one diagram, or in the absence of independent support, is treated as a tentative affinity rather than a definitive correlation.

Our approach follows previous work showing that mineral chemistry can complement lithofacies, petrography, geochronology, and stratigraphy in the correlation of ignimbrites and tephra deposits [e.g. Hildreth and Mahood 1985; de Silva and Francis 1989; Lindsay et al. 2001; Shane et al. 2003; Folkes et al. 2011; Smith et al. 2011; Breitkreuz et al. 2014]. In particular, Fe–Mg relationships and Mg# have been widely used as discriminants in glass and mineral chemistry correlation studies [e.g. Shane et al. 2003; Smith et al. 2011]. Therefore, in addition to oxide vs. SiO_2 diagrams, we compare selected units using FeO vs. MgO and Mg# vs. TiO_2 plots (Figure 8). Mg# is defined here as $Mg/(Mg + Fe_{total})$, calculated on a molar basis from structural-formula cations, where Fe_{total} represents total iron.

This strategy is consistent with broader tephrochronological approaches in which correlations are strengthened by combining geochemical fingerprints with independent stratigraphic, chronological, and petrographic constraints. In many studies, glass major- and trace-element compositions provide the most powerful correlation tool, particularly when individual glass shards can be analyzed by EPMA and LA-ICP-MS [e.g. Pearce et al. 2007; Lowe et al. 2017]. However, where glass is altered, absent, compositionally overlapping, or diffi-

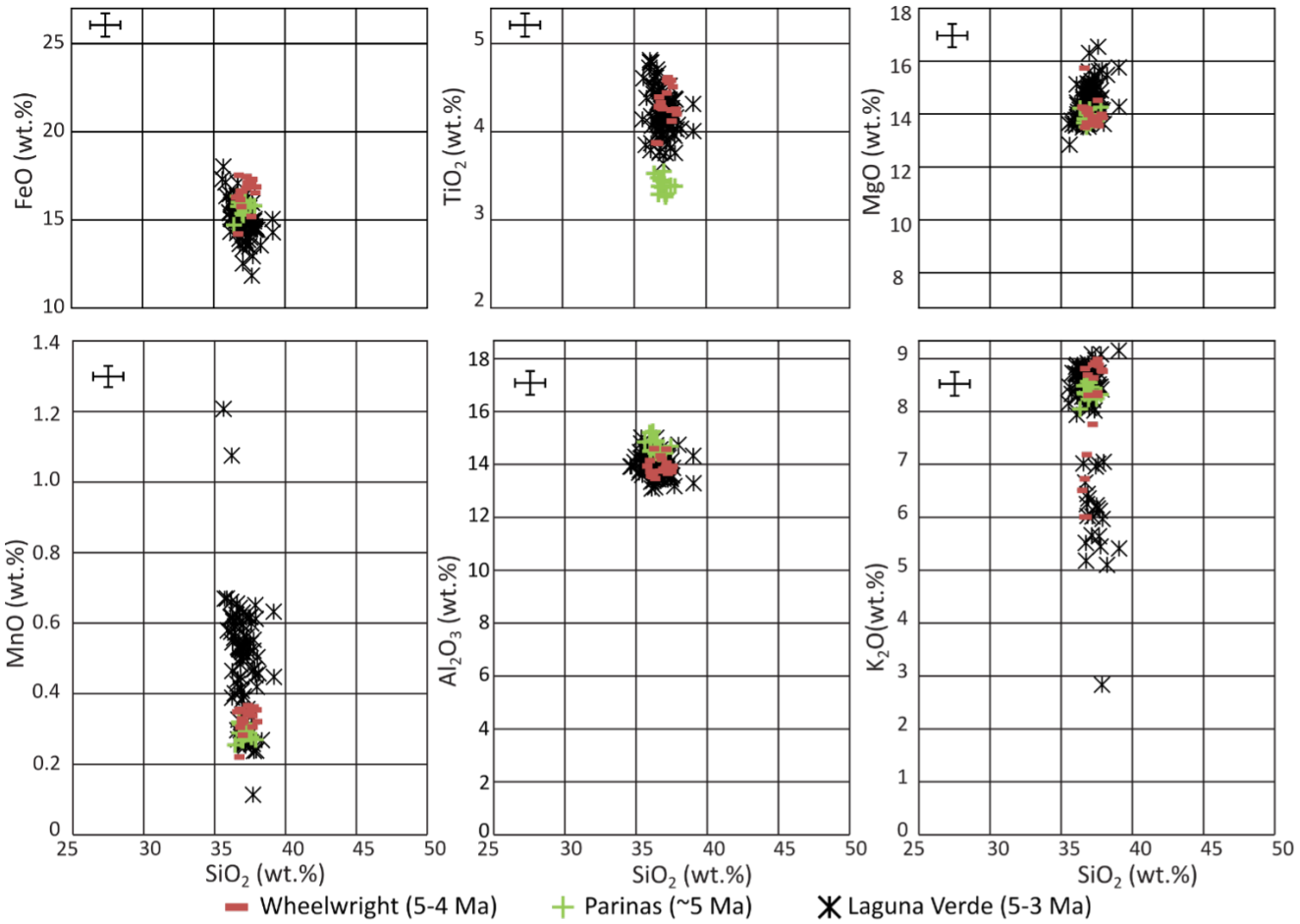


Figure 7: Distribution of different major elements as a function of silica content, expressed as weight percentage of oxides (wt.%), for biotite analyses from the Wheelwright, Parinas, and Laguna Verde ignimbrites. Bars in the upper-left corner of each graph represent maximum estimated uncertainties.

cult to compare between proximal and distal deposits, mineral chemistry can provide an important complementary or alternative fingerprint. Examples include the use of biotite chemistry for the Toba tephra and other Quaternary tephra deposits [Shane et al. 2003; Smith et al. 2011], and trace-element compositions of biotite for distinguishing magma batches in volcanic systems [Sliwinski et al. 2017]. In this context, our dataset provides a first regional biotite major-element reference framework for testing correlations among southern CVZ ignimbrites and between Andean ignimbrites and distal ashfall deposits.

4.2 Río Frío–Vega Helada Differentiation

As summarized above, Río Frío and Vega Helada are physically similar and partly overlap in age, making them difficult to separate using field and geochronological criteria alone.

Despite these similarities, their biotite compositions define distinct fields in the major-element diagrams (Figure 5). This distinction is also evident in the FeO vs. MgO diagram, where Vega Helada biotites are generally richer in FeO and poorer in MgO than Río Frío biotites (Figure 8A). Similarly, Mg# vs. TiO_2 systematics show that Río Frío and Vega Helada occupy different compositional fields, with Vega Helada characterized by slightly lower Mg# but notably lower TiO_2 values (Figure 8C). These differences indicate that the two units can be distinguished using biotite chemistry, even where field characteristics and published ages are similar.

4.3 Pajonales–Juncalito Correlation

As summarized in the results section, Pajonales and Juncalito ignimbrites share fibrous pumice-rich facies, low crystal contents, coarse shard-rich matrices, and overlapping ages.

Their biotite compositions overlap broadly in the oxide vs. SiO_2 diagrams (Figure 5), and this similarity is also clear in FeO vs. MgO and Mg# vs. TiO_2 diagrams (Figure 8B,D). In the FeO vs. MgO plot, analyses from both units occupy the same general compositional field, without a clear separation between them (Figure 8B). Similarly, Mg# vs. TiO_2 values overlap substantially, supporting a close geochemical affinity between Pajonales and Juncalito (Figure 8D). Together with their similar lithofacies, petrography, and compatible ages, these results support a close correlation between both units. Juncalito may represent the southernmost and westernmost preserved deposits of the Pajonales Ignimbrite or, alternatively, both units may correspond to closely related eruptive events from the same magmatic system.

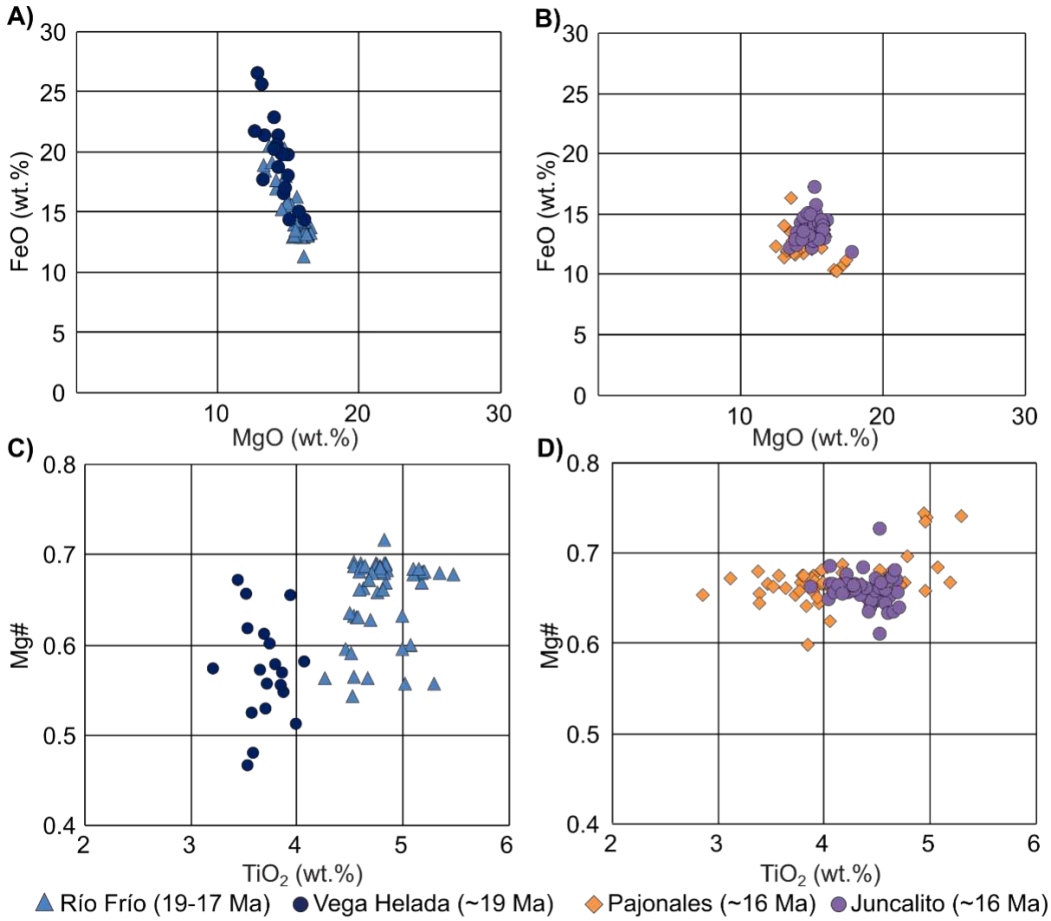


Figure 8: Specific biotite chemistry comparison diagrams for the main proximal correlation issues discussed in this study. [A] FeO vs. MgO diagram comparing the Río Frío (RF) and Vega Helada (VH) ignimbrites. [B] FeO vs. MgO diagram comparing the Pajonales (PAJ) and Juncalito (Junc) ignimbrites. [C] Mg# vs. TiO_2 diagram for Río Frío and Vega Helada. [D] Mg# vs. TiO_2 diagram for Pajonales and Juncalito. Mg# is defined as Mg/(Mg + Fe_{total}), calculated on a molar basis from structural-formula cations, where Fe_{total} represents total iron. Oxide concentrations are expressed in wt.%.

4.4 Distal Ash-Fall Correlation

A key objective of this study is to evaluate whether biotite chemistry can be used to link proximal ignimbrites of the southern CVZ with distal ash-fall deposits preserved in the Coastal Cordillera. Breitkreuz et al. [2014] analyzed several Neogene to Quaternary ash deposits near the northern Chilean coast and compared them with large ignimbrites from the Altiplano Puna Volcanic Complex, to the north of our study area. However, some of their primary fall deposits could not be confidently linked to a specific source unit. Here, we compare our biotite data with the primary fall deposits L1, L4, L7, L8, L9, and L11 of Breitkreuz et al. [2014]. Reworked deposits were excluded to minimize the possibility of mixed or contaminated signals. Because the distal deposits reported by Breitkreuz et al. [2014] are younger than ~7 Ma, the comparison was restricted to the younger ignimbrites in our dataset: Wheelwright, Parinas, and Laguna Verde.

Following the approach of Breitkreuz et al. [2014], we compare the same biotite compositional parameters used in their study : Mn, Al(iv), Ti, and Mg/Fe, all expressed as a.p.f.u. Correlations are considered strong only when chemical overlap is accompanied by compatible age constraints; otherwise, they are treated as tentative affinities. The strongest correlation is observed between sample L9 of Breitkreuz et al. [2014] and the Laguna Verde Ignimbrite (Figure 9). The biotite compositions overlap in the main discrimination diagrams, and the reported age of L9, 3.91 ± 0.10 Ma, is compatible with the published age range of the Laguna Verde Ignimbrite. This combined geochemical and chronological agreement supports the interpretation that L9 represents a distal ash-fall deposit associated with the Laguna Verde eruptive event.

Sample L4 shows a possible affinity with the Wheelwright Ignimbrite (Figure 9). However, this correlation is less robust than the L9–Laguna Verde correlation because it relies mainly on biotite chemistry and lacks the same level of independent chronological support. We therefore interpret L4 as a tentative match with Wheelwright rather than a definitive correlation. The remaining distal ash-fall localities analyzed by Breitkreuz et al. [2014] do not show consistent overlap with the Wheelwright, Parinas, or Laguna Verde ignimbrites in the diagrams considered here. Given the ~350 km transport distance, these deposits are interpreted as fall deposits rather than direct pyroclastic density current deposits, consistent with their original description by Breitkreuz et al. [2014].

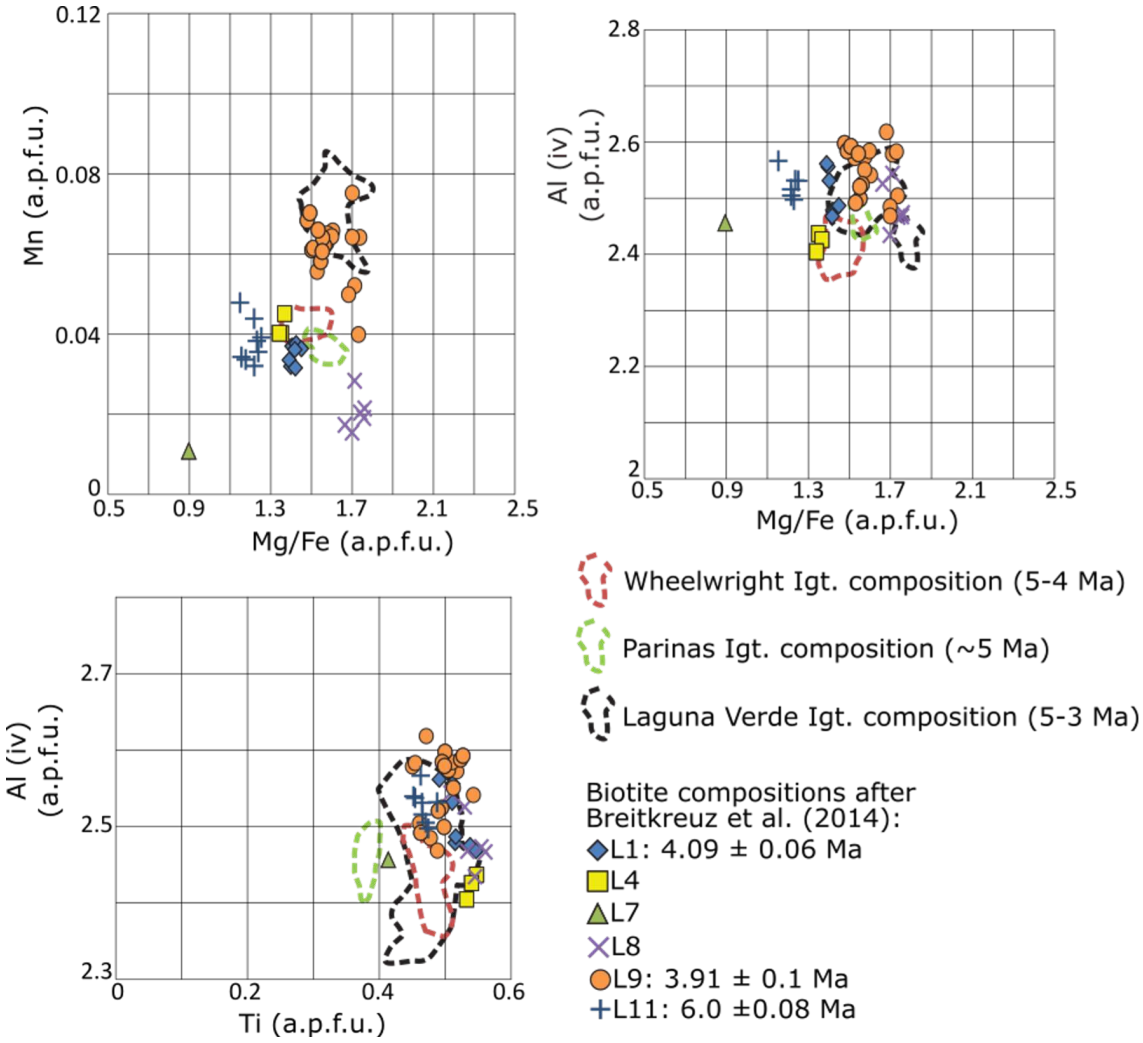


Figure 9: Comparison between biotite chemistry from the Wheelwright, Parinas, and Laguna Verde ignimbrites and published biotite data from distal ash-fall deposits in the Coastal Cordillera near Antofagasta [Breitkreuz et al. 2014]. The diagrams follow the same compositional parameters used by Breitkreuz et al. [2014]. Colored dashed outlines represent the compositional ranges of the ignimbrites analyzed in this study.

These results show that biotite chemistry can be useful not only for distinguishing proximal ignimbrite units, but also for testing source-to-distal correlations where glass chemistry, field continuity, or direct stratigraphic tracing are unavailable. Nevertheless, distal correlations should be considered most reliable when mineral chemistry is combined with independent age constraints and stratigraphic or geographic plausibility.

4.5 Future Perspectives

Although this study focuses on biotite chemistry as a fingerprinting tool for ignimbrite and distal ash-fall correlation, some compositional patterns observed in the dataset may have broader petrological significance. For example, the high internal variability of biotite chemistry in the Vega Helada and Los Colorados ignimbrites (Figure 5, Figure 6) could reflect complex crystal populations, magma recharge, crystal recycling, or compositional zoning within their magmatic systems. Similar processes have been documented in other large silicic systems, including the Bishop Tuff and Cerro Galán Ignimbrite [e.g. Hildreth and Wilson 2007; Wark et al. 2007; Wright et al. 2011]. Likewise, systematic differences in Ti content between some units or subunits may record variations in crystallization conditions, as Ti in biotite has been linked to temperature in several studies [e.g. Zhang et al. 2016]. For instance, the progressive decrease in Ti content from the older Río Frío Ignimbrite to the younger San Andrés Ignimbrite, broadly following the Aguilar–Salar Grande–Barrancas Blancas–Pampa de Los Bayos caldera trend, could be explored as a possible indication of changing crystallization conditions, although this remains only a preliminary observation.

Testing these hypotheses would require dedicated petrological studies integrating additional mineral phases, glass chemistry, whole-rock geochemistry, trace-element mineral chemistry, and phase-equilibrium approaches. In particular, geothermobarometric studies, independent oxybarometry, and detailed core-to-rim or population-scale analyses of biotite and coexisting minerals would be necessary to evaluate whether the observed chemical variations reflect pre-eruptive

magma conditions, crystal recycling, or syn-eruptive mixing and transport processes. We therefore treat these observations as preliminary indications and identify them as promising directions for future work rather than as conclusions of the present study.

4.6 Conclusions

The major-element chemistry of biotite crystals from twelve Neogene ignimbrites of the southern Central Andean Volcanic Zone was characterized using EPMA. Most units define distinctive compositional fields, supporting the use of biotite chemistry as an effective fingerprinting tool for ignimbrite correlation in northern Chile.

Biotite chemistry distinguishes the Río Frío and Vega Helada ignimbrites, despite their similar lithofacies, petrographic features, and partially overlapping published age ranges. In contrast, the Pajonales and Juncalito ignimbrites show overlapping biotite compositions, similar petrographic characteristics, and compatible ages, supporting a close correlation between them. Juncalito may represent the southernmost and westernmost preserved deposits of the Pajonales Ignimbrite, or both units may correspond to closely related eruptive events from the same magmatic system.

Comparison with published biotite data from distal ash-fall deposits in the Coastal Cordillera near Antofagasta suggests that locality L9 of Breitkreuz et al. [2014] can be correlated with the Laguna Verde Ignimbrite, supported by both biotite chemistry and compatible age constraints. Locality L4 shows a possible affinity with the Wheelwright Ignimbrite, although this correlation remains more tentative because it relies mainly on biotite chemistry.

These results show that biotite chemistry is most powerful when integrated with independent constraints such as stratigraphy, petrography, field relationships, geochronology, and geographic distribution. This multi-proxy approach is particularly useful where ignimbrites have similar field characteristics, discontinuous exposure, uncertain sources, or overlapping age ranges.

Some compositional patterns observed in the dataset, such as the high internal variability of Vega Helada and Los Colorados or systematic Ti differences among some units, may have petrological significance. However, these aspects require additional datasets and dedicated petrological studies and are therefore treated here only as future research directions, not as conclusive results.

Author Contributions

Francisco Hevia-Cruz: conceptualization, methodology, validation, data curation, investigation, writing (original draft, reviewing and edition) and visualization. **José A. Naranjo**: conceptualization, validation, investigation, writing (reviewing and edition), and supervision. **Yuji Orihashi**: validation, investigation, writing (reviewing and edition), supervision, and funding acquisition.

Acknowledgements

This work was partially funded by Project No. 8011 of the National Geology Plan of SERNAGEOMIN, which supported the field campaigns, preparation of thin sections, petrographic studies, and the preparation of biotite concentrates. The University of Tokyo provided significant financial support for this study by granting access to its facilities for mineral geochemistry analysis via Electron Probe Microanalyzer and covering a one-month stay for conducting these analyses, for which we especially thank Professors Ryo Anma, Daiji Hirata, and Atsushi Yasuda, as well as Natsumi Hokanishi for technical support. We thank Adriano Pimentel, two anonymous reviewers, and the editor, Adam Jeffery, for their constructive comments and helpful suggestions, which significantly improved this work.

Data Availability

All data used in this work can be found in the Supplementary Material. Appendix A1 corresponds to field and thin section images that support descriptions and facies distribution and correlations; Appendix A2 corresponds to the used geochronological data presented as a table (Supplementary Table ST1); and Appendix A3 corresponds to the geochemical data (Supplementary Table ST2) and graphics for biotite and magma classification. References cited only in the Supplementary Material are listed in Appendix A4.

Copyright Notice

© The Author(s) 2026. This article is distributed under the terms of the Creative Commons Attribution 4.0 International License, which permits unrestricted use, distribution, and reproduction in any medium, provided you give appropriate credit to the original author(s) and the source, provide a link to the Creative Commons license, and indicate if changes were made.

References

Branney, M. and P. Kokelaar (2002). "Pyroclastic density currents and the sedimentation of ignimbrites". Volume 27. Geological Society of London. ISBN: 978-1862394025. DOI: 10.1144/GSL.MEM.2003.027.

Breitkreuz, C., S. L. de Silva, H. G. Wilke, J. A. Pfänder, and A. D. Renno (2014). "Neogene to Quaternary ash deposits in the Coastal Cordillera in northern Chile: Distal ashes from supereruptions in the Central Andes". *Journal of Volcanology and Geothermal Research* 269, pages 68–82. DOI: 10.1016/j.jvolgeores.2013.11.001.

Clark, A. H., A. E. S. Mayer, C. Mortimer, R. H. Sillitoe, R. U. Cooke, and N. J. Snelling (1967). "Implications of the Isotopic Ages of Ignimbrite Flows, Southern Atacama Desert, Chile". *Nature* 215(5102), pages 723–724. DOI: 10.1038/215723a0.

Clavero, J., C. Mpodozis, and M. Gardeweg (1997). "Mapa Geológico Preliminar del área del Salar de Wheelwright, Región de Atacam (escala 1:100.000)". Servicio Nacional de Geología y Minería.

Clavero, J., C. Mpodozis, M. Gardeweg, and M. Valenzuela (2012). "Geología de las áreas Laguna Wheelwright y Paso San Francisco, Región de Atacama. (escala 1:100.000)". *Carta Geológica de Chile*. 139-140. Servicio Nacional de Geología y Minería.

De Silva, S. and P. Francis (1989). "Correlation of large ignimbrites — Two case studies from the Central Andes of northern Chile". *Journal of Volcanology and Geothermal Research* 37(2), pages 133–149. DOI: 10.1016/0377-0273(89)90066-8.

Deer, W., R. Howie, and J. Zussman (1992). *An Introduction to the Rock Forming Minerals*. Second Edition. Pearson. ISBN: 978-0582300941.

Droop, G. T. R. (1987). "A general equation for estimating Fe^{3+} concentrations in ferromagnesian silicates and oxides from microprobe analyses, using stoichiometric criteria". *Mineralogical Magazine* 51(361), pages 431–435. DOI: 10.1180/minmag.1987.051.361.10.

Dunai, T. J., G. A. González López, and J. Juez-Larré (2005). "Oligocene–Miocene age of aridity in the Atacama Desert revealed by exposure dating of erosion-sensitive landforms". *Geology* 33(4), pages 321–324. DOI: 10.1130/g21184.1.

Folkes, C. B., S. L. de Silva, H. M. Wright, and R. A. F. Cas (2011). "Geochemical homogeneity of a long-lived, large silicic system; evidence from the Cerro Galán caldera, NW Argentina". *Bulletin of Volcanology* 73(10), pages 1455–1486. DOI: 10.1007/s00445-011-0511-y.

Hildreth, W. and G. Mahood (1985). "Correlation of ash-flow tuffs". *Geological Society of America Bulletin* 96(7), pages 968–974. DOI: 10.1130/0016-7606(1985)96<968:coat>2.0.co;2.

Hildreth, W. and C. J. N. Wilson (2007). "Compositional Zoning of the Bishop Tuff". *Journal of Petrology* 48(5), pages 951–999. DOI: 10.1093/petrology/egm007.

Lindsay, J., S. de Silva, R. Trumbull, R. Emmermann, and K. Wemmer (2001). "La Pacana caldera, N. Chile: a re-evaluation of the stratigraphy and volcanology of one of the world's largest resurgent calderas". *Journal of Volcanology and Geothermal Research* 106(1-2), pages 145–173. DOI: 10.1016/s0377-0273(00)00270-5.

Lowe, D. J., N. J. Pearce, M. A. Jorgensen, S. C. Kuehn, C. A. Tryon, and C. L. Hayward (2017). "Correlating tephras and cryptotephras using glass compositional analyses and numerical and statistical methods: Review and evaluation". *Quaternary Science Reviews* 175, pages 1–44. DOI: 10.1016/j.quascirev.2017.08.003.

Naranjo, J. A. and P. Cornejo (1992). "Hoja Salar de la Isla, Regiones de Antofagasta y Atacama". *Carta Geológica de Chile*. 72. Servicio Nacional de Geología y Minería.

Naranjo, J. A. and A. Puig (1984). "Hojas Taltal y Chañaral (escala 1:250.000)". *Carta Geológica de Chile*. 62-63. Servicio Nacional de Geología y Minería.

Naranjo, J. A., C. Ramírez, and V. Villa (2016). "Geología de las áreas Cerro Panteón de Aliste y Cerro Colorado, Región de Atacama (escala 1:100.000)". *Carta Geológica de Chile*. Servicio Nacional de Geología y Minería.

Naranjo, J. A., V. Villa, and C. Venegas (2013a). "Geología de las áreas Salar de Aguilar y Portezuelo del León Muerto, Región de Atacama (escala 1:100.000)". *Carta Geológica de Chile*. 151-152. Servicio Nacional de Geología y Minería.

– (2013b). "Geología de las áreas Salar de Pajonales y Cerro Moño, regiones de Antofagasta y Atacama (escala 1:100.000)". *Carta Geológica de Chile*. 153-154. Servicio Nacional de Geología y Minería.

Naranjo, J. A., F. Hevia, V. Villa, and C. A. Ramírez (2019). "Miocene to Holocene geological evolution of the Lazufre segment in the Andean volcanic arc". *Geosphere* 15(1), pages 47–59. DOI: 10.1130/ges01352.1.

Naranjo, J. A., V. Villa, C. Ramírez, and C. Pérez de Arce (2018). "Volcanism and tectonism in the southern Central Andes: Tempo, styles, and relationships". *Geosphere* 14(2), pages 626–641. DOI: 10.1130/ges01350.1.

Pearce, N. J. G., J. S. Denton, W. T. Perkins, J. A. Westgate, and B. V. Alloway (2007). "Correlation and characterisation of individual glass shards from tephra deposits using trace element laser ablation ICP-MS analyses: current status and future potential". *Journal of Quaternary Science* 22(7), pages 721–736. DOI: 10.1002/jqs.1092.

Rieder, M., G. Cavazzini, Y. S. D'yakonov, V. A. Frank-Kamenetskii, G. Gottardi, S. Guggenheim, P. W. Koval', G. Müller, A. M. R. Neiva, E. W. Radoslovich, J.-L. Robert, F. P. Sassi, H. Takeda, Z. Weiss, and D. R. Wones (1998). "Nomenclature of the Micas". *Clays and Clay Minerals* 46(5), pages 586–595. DOI: 10.1346/ccmn.1998.0460513.

Schnurr, W., R. Trumbull, J. Clavero, K. Hahne, W. Siebel, and M. Gardeweg (2007). "Twenty-five million years of silicic volcanism in the southern central volcanic zone of the Andes: Geochemistry and magma genesis of ignimbrites from 25 to 27 °S, 67 to 72 °W". *Journal of Volcanology and Geothermal Research* 166(1), pages 17–46. DOI: 10.1016/j.jvolgeores.2007.06.005.

Seggiaro, R., R. Becchio, F. Pereyra, and L. Martinez (2007). "Hoja Geológica 2569-IV. Antofalla, provincias de Catamarca y Salta (escala 1:250.000)". *Instituto de Geología y Recursos Minerales Boletines*. 343. Servicio Geológico y Minero Argentino.

Seggiaro, R. E., F. D. Hongn, A. Castillo, F. Pereyra, D. Villegas, and L. Martínez (2006). "Hoja Geológica 2769-II, Paso San Francisco (escala 1:250.000)". *Instituto de Geología y Recursos Minerales Boletines*. 294. Servicio Geológico y Minero Argentino.

Shane, P., V. Smith, and I. Nairn (2003). "Biotite composition as a tool for the identification of Quaternary tephra beds". *Quaternary Research* 59(2), pages 262–270. DOI: 10.1016/s0033-5894(03)00012-7.

Siebel, W., W. B. Schnurr, K. Hahne, B. Kraemer, R. B. Trumbull, P. van den Bogaard, and R. Emmermann (2001). "Geochemistry and isotope systematics of small- to medium-volume Neogene–Quaternary ignimbrites in the southern central Andes: evidence for derivation from andesitic magma sources". *Chemical Geology* 171(3-4), pages 213–237. DOI: 10.1016/s0009-2541(00)00249-7.

Sliwinski, J. T., B. S. Ellis, P. Dávila-Harris, J. A. Wolff, P. H. Olin, and O. Bachmann (2017). "The use of biotite trace element compositions for fingerprinting magma batches at Las Cañadas volcano, Tenerife". *Bulletin of Volcanology* 79(1). DOI: 10.1007/s00445-016-1088-2.

Smith, V. C., N. J. Pearce, N. E. Matthews, J. A. Westgate, M. D. Petraglia, M. Haslam, C. S. Lane, R. Korisettar, and J. Pal (2011). "Geochemical fingerprinting of the widespread Toba tephra using biotite compositions". *Quaternary International* 246(1-2), pages 97–104. DOI: 10.1016/j.quaint.2011.05.012.

Speer, J. . A. (1984). "Micas in igneous rocks". *Reviews in Mineralogy: Micas*. Edited by S. Bailey. Volume 13, pages 299–356. DOI: 10.1515/9781501508820-013.

Stern, C. R. (2004). "Active Andean volcanism: its geologic and tectonic setting". *Revista geológica de Chile* 31(2), pages 161–206. DOI: 10.4067/s0716-02082004000200001.

Wark, D., W. Hildreth, F. Spear, D. Cherniak, and E. Watson (2007). "Pre-eruption recharge of the Bishop magma system". *Geology* 35(3), pages 235–238. DOI: 10.1130/g23316a.1.

Whitney, D. and B. Evans (2010). "Abbreviations for names of rock-forming minerals". *American Mineralogist* 95(1), pages 185–187. DOI: 10.2138/am.2010.3371.

Wright, H. M. N., C. B. Folkes, R. A. F. Cas, and K. V. Cashman (2011). "Heterogeneous pumice populations in the 2.08-Ma Cerro Galán Ignimbrite: implications for magma recharge and ascent preceding a large-volume silicic eruption". *Bulletin of Volcanology* 73(10), pages 1513–1533. DOI: 10.1007/s00445-011-0525-5.

Zhang, W., D. R. Lentz, K. G. Thorne, and C. McFarlane (2016). "Geochemical characteristics of biotite from felsic intrusive rocks around the Sisson Brook W–Mo–Cu deposit, west-central New Brunswick: An indicator of halogen and oxygen fugacity of magmatic systems". *Ore Geology Reviews* 77, pages 82–96. DOI: 10.1016/j.oregeorev.2016.02.004.